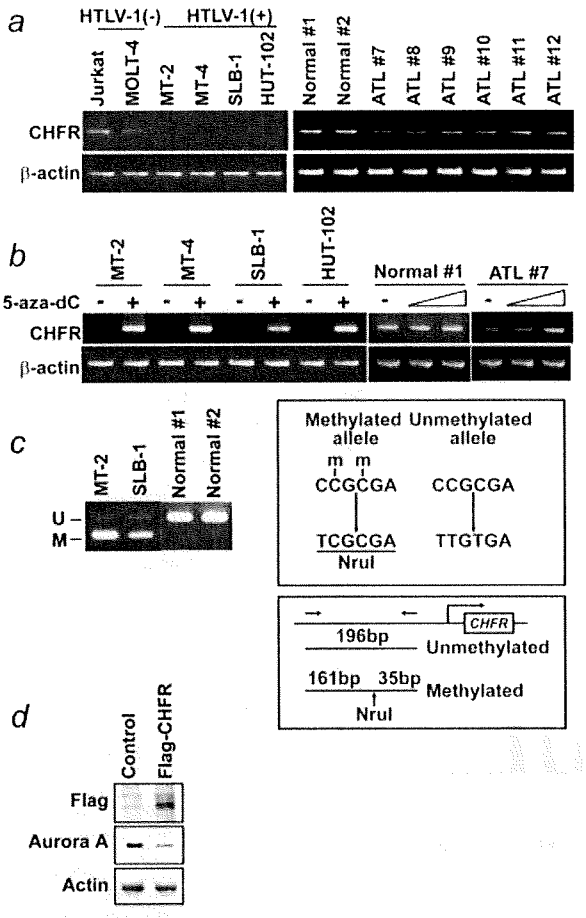

FIGURE 2 – Loss of CHFR expression by aberrant methylation is associated with accumulation of Aurora A. (*a*) CHFR mRNA expression in HTLV-1-infected T-cell lines [HTLV-1(+)], uninfected T-cell lines [HTLV-1(−)], PBMCs from patients with ATL (ATL 7–12), and those from healthy donors (Normal 1 and 2) was analyzed by RT-PCR. β-actin expression was a control for cDNA synthesis. (*b*) Re-expression of CHFR mRNA in HTLV-1-infected T-cell lines and PBMCs from a patient with ATL, after treatment with 5-aza-dC, a methyltransferase inhibitor. Cells were treated with (+) or without (−) 5-aza-dC (2 μM) for 48 hr (cell lines). PBMCs from a patient with ATL (ATL 7) and a healthy donor (Normal 1) were treated with increasing amount of 5-aza-dC (0, 1 or 2 μM) for 48 hr. The expression of CHFR mRNA was analyzed by RT-PCR. (*c*) Bisulfite treatment and COBRA of the *CHFR* CpG islands in MT-2 and SLB-1 cells and PBMCs from healthy donors (Normal 1 and 2). *M*, methylated alleles; U, unmethylated alleles (left panels). Schematic representations of COBRA assay (right panels). After bisulfite treatment, the PCR products, which contain an NruI restriction site that recognizes TCGCGA, were digested only when CpG sites were retained because of methylation (upper right). The PCR products from unmethylated alleles were 196-bp and methylated alleles were 161- and 35-bp in size (lower right) (*d*) HUT-102 cells were transfected with Flag-tagged CHFR expression plasmid (Flag-CHFR) or control vector (Control). Cells were harvested 48 hr after transfection. The expression levels of transfected CHFR (Flag) and Aurora A were analyzed by western blotting. Actin expression served as a control. Representative results of three experiments with similar findings.

were not as dramatic as HTLV-1-infected T-cell lines, because PBMCs included normal cells which express high levels of CHFR. Is the loss of *CHFR* gene expression in HTLV-1-infected T-cell lines due to aberrant methylation of the promoter of this gene? To answer this question, we treated HTLV-1-infected T-cell lines with DNA methyltransferase inhibitor, 5-aza-dC, which interferes with DNA methylation. Such treatment restored *CHFR* gene expression, suggesting the silencing of *CHFR* gene in HTLV-1-infected T-cell lines was methylation-dependent (Fig. 2*b*). We also found that 5-aza-dC enhanced *CHFR* gene expression in primary ATL cells but not in PBMCs from a healthy donor (Fig. 2*b*). To further investigate the relationship between methylation of CpG island in *CHFR* promoter and expression of this gene expression, we used COBRA to survey the methylation status of individual CpG dinucleotides within the *CHFR* gene in HTLV-1-infected T-cell lines and PBMCs from healthy donors (Fig. 2*c*). Using a set of primers that encompass the region surrounding the putative transcription start site, we found HTLV-1-infected T-cell lines that harbored densely methylated CpG sites, and PBMCs from healthy donors that did not exhibit any detectable methylation (Fig. 2*c*, left panel), indicating that the 5′ CpG island of *CHFR* gene is aberrantly methylated in HTLV-1-infected T-cell lines. Unfortunately, we did not have enough PBMC samples from ATL patients to analyze methylation status. To confirm the link between CHFR and Aurora A expression in HTLV-1-infected T-cell lines, Flag-tagged CHFR expression plasmid was transfected into HUT-102 cells (Fig. 2*d*). Transient expression of CHFR reduced Aurora A protein levels in HUT-102 cells, suggesting that loss of CHFR seems to stabilize Aurora A protein in HTLV-1-infected T-cell lines.

Knockdown of Aurora A suppresses cell growth and NF-κB signaling in an HTLV-1-infected T-cell line

To analyze the effect of Aurora A on the growth of HTLV-1-infected T cells, we knocked down Aurora A expression in HUT-102 cells by siRNA. Lack of Aurora A expression suppressed the growth of HUT-102 cells, compared with Aurora A-expressing HUT-102 cells transfected with control siRNA (Fig. 3*a*, upper left panel). We confirmed that siRNA specifically knocked down Aurora A and did not affect Aurora B (Fig. 3*b*). We also found that CHFR transfection in HUT-102 cells markedly inhibited cell growth compared with transfection of empty vector (Fig. 3*a*, upper right panel). On the other hand, the effects of Aurora A siRNA and CHFR transfection were smaller in Jurkat cells than those in HUT-102 cells (Fig. 3*a*, lower panels). Does Aurora A knockdown influence NF-κB signaling pathway? This is important because constitutively activated NF-κB signaling plays important roles in the growth and survival of HTLV-1-infected T cells.[36,40] Aurora A siRNA reduced phosphorylation of IKKβ, but not that of IKKα and IKKγ, without affecting Tax expression in HUT-102 cells (Fig. 3*b* and data not shown). Reporter assay showed that Aurora A enhanced Tax-induced NF-κB transcriptional activity but kinase dead mutant of Aurora A did not change that activity (Fig. 3*c*, left panel). However, without Tax both wild type and kinase dead mutant of Aurora A could not activate NF-κB reporter (Fig. 3*c*, right panel). Transient transfection assay using NF-κB reporter and CHFR expression plasmid (Fig. 3*d*, left panel) or Aurora A siRNA (Fig. 3*d*, right panel) showed that CHFR expression or Aurora A knockdown suppressed constitutive NF-κB activity in HUT-102 cells.

Aurora kinase inhibitor induces apoptosis of HTLV-1-infected T-cells

Next, we examined the effects of Aurora kinase inhibitor on the growth of HTLV-1-infected T-cell lines. In this study, we were forced to use a pan-Aurora kinase inhibitor known to inhibit both Aurora A and B[41] because no specific Aurora A inhibitor is available commercially. The pan-Aurora kinase inhibitor reduced the cell number of HUT-102 but induced growth arrest rather than decreased cell number of Jurkat cells (Fig. 4*a*, left panel). Importantly, Aurora kinase inhibitor also reduced the viability of PBMCs from patients with ATL but not those from healthy donors (Fig. 4*a*, right panel). Because of the lack of adequate ATL samples, we could not analyze the expression of Aurora A protein in

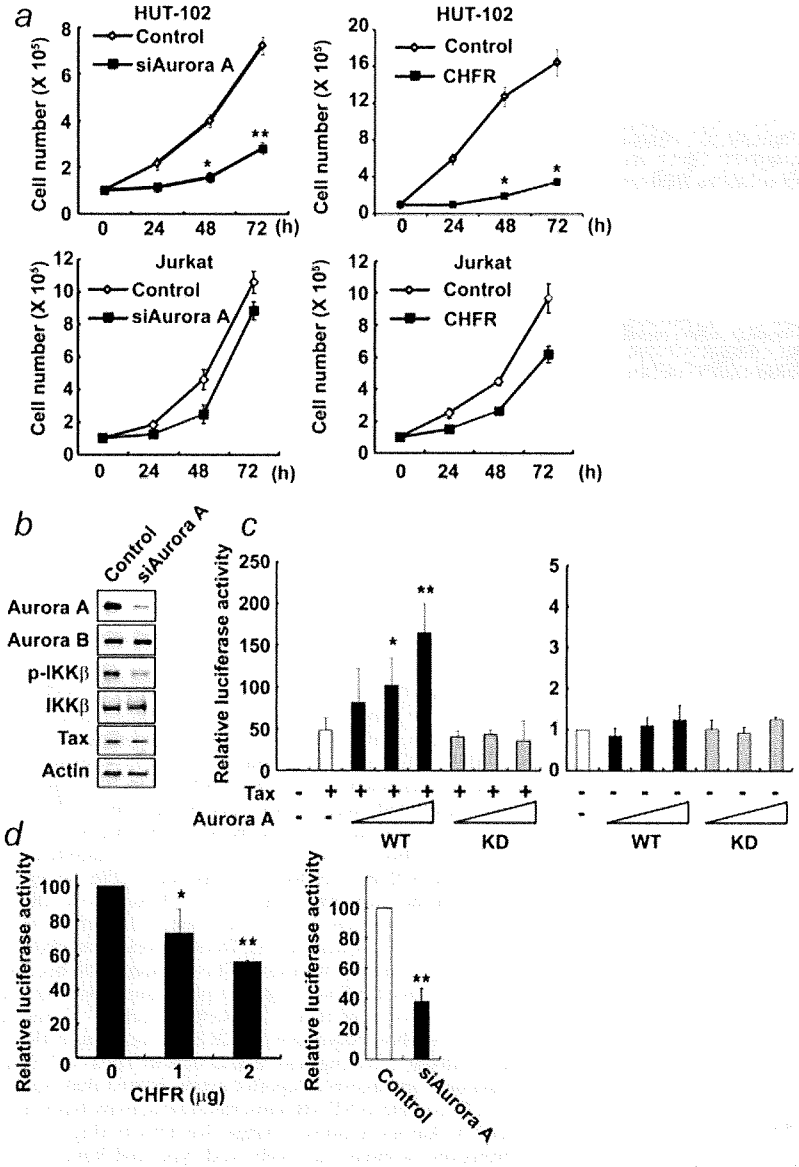

FIGURE 3 – Knockdown of Aurora A suppresses the growth and NF-κB signaling of an HTLV-1-infected T-cell line. (*a*) HUT-102 (upper panels) or Jurkat (lower panels) cells were transfected with 100 nM siRNA targeting Aurora A (left panels) or 2 μg of CHFR expression plasmid (right panels). Cells were cultured for the indicated time periods. Viable cell numbers were counted in triplicate by trypan blue dye exclusion method. Data are mean ± SD of viable cell numbers (*$p < 0.01$, **$p < 0.0005$). (*b*) Cell lysates prepared from HUT-102 cells 24 hr after transfection of Aurora A siRNA were analyzed by western blotting with the indicated antibodies. (*c*) Aurora A enhanced Tax-induced NF-κB activity. Jurkat cells were transfected with Tax expression plasmid or empty vector (0.1 μg) and NF-κB reporter plasmid (κB-LUC; 0.1 μg), together with increasing amount (0, 0.5, 1 or 2 μg) of either Aurora A wild type (WT) or Aurora A kinase dead mutant (KD) as indicated in the figure. Cells were harvested 48 hr after transfection. Luciferase activity was analyzed as described in "Material and methods" section. Data are mean ± SD of triplicate experiments. The activity was expressed relative to that of cells transfected with reporter plasmid alone, which was defined as 1 (*$p < 0.05$, **$p < 0.01$). (*d*) CHFR or Aurora A siRNA inhibited NF-κB activity in an HTLV-1-infected T-cell line. HUT-102 cells were transfected with κB-LUC together with increasing amount of CHFR expression plasmids (left panel) or 100 nM Aurora A siRNA (right panel). Cells were harvested 48 hr after transfection. Luciferase activity was analyzed as described in "Material and methods" section. Data are mean ± SD of triplicate experiments. The activity was expressed relative to that of cells transfected with reporter alone, which was defined as 100 (*$p < 0.05$, **$p < 0.0005$).

these Aurora kinase inhibitor-treated ATL samples. Exposure of Jurkat cells to Aurora kinase inhibitor resulted in marked increase of 8N DNA content in the cells due to inhibition of cell division (Fig. 4*b*, left panel). Interestingly, exposure of HUT-102 cells to Aurora kinase inhibitor did not increase cells 8N DNA content (Fig. 4*b*, right panel). Exposure of HTLV-1-infected T-cell lines to Aurora kinase inhibitor for 24 hr increased the number of apoptotic cells. In contrast, apoptotic cells were barely increased in HTLV-1-uninfected T-cell lines (Fig. 4*c*). Cleaved form of PARP, marker of apoptosis, was increased in HUT-102 cells but not in Jurkat and MOLT-4 cells treated with Aurora kinase inhibitor (Fig. 4*d*).

Aurora kinase inhibitor suppresses NF-κB activity in HTLV-1-infected T-cells

Finally, we examined the effects of Aurora kinase inhibitor on NF-κB activity in HUT-102 cells. The inhibitor reduced the transcriptional activity of NF-κB in HUT-102 cells, as revealed by the reporter assay (Fig. 5*a*), and inhibited the DNA binding of NF-κB, but not that of AP-1 (which is also activated by HTLV-1 infection) (Fig. 5*b*). Similar to Aurora A knockdown experiments (Fig. 3*b*), Aurora kinase inhibitor reduced phosphorylation of IKKβ (Fig. 5*c*), but not that of IKKα and IKKγ (data not shown). Reduced phosphorylation resulted in reduced phosphorylation and increased accumulation of IκBα, a downstream phosphorylation target of IKK complex (Fig. 5*c*). Aurora kinase inhibitor also reduced the expression of antiapoptotic protein, survivin (Fig. 5*c*), which is induced by Tax through activation of NF-κB pathway.[42]

Discussion

In the present study, we reported the presence of high expression levels of Aurora A protein in HTLV-1-infected T-cell lines than in uninfected T-cell lines, and in primary ATL cells than in normal PBMCs. These results are in agreement with the recent study of Ikezoe *et al.*[43] who showed aberrant expression of Aurora

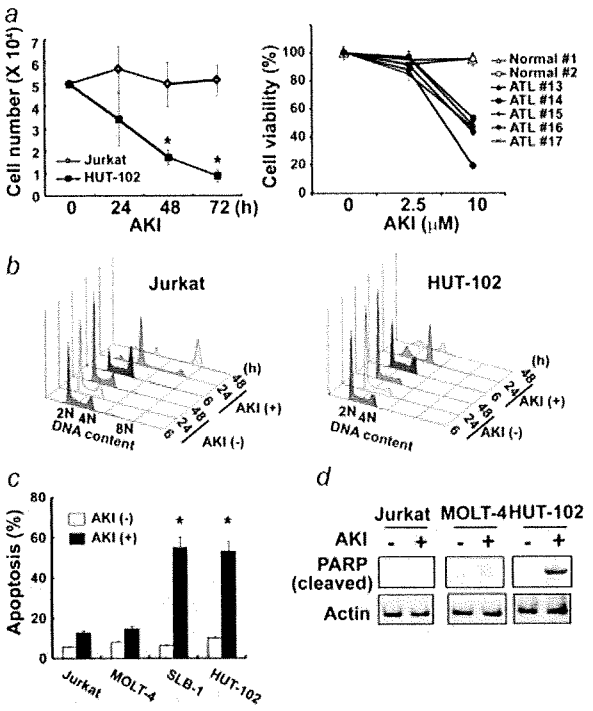

FIGURE 4 – Aurora kinase inhibitor induces cell death in HTLV-1-infected T-cell lines and primary ATL cells. (*a*) Left panel; Jurkat and HUT-102 cells were treated with Aurora kinase inhibitor (AKI) (10 μM) for the indicated time periods. The number of viable cells was counted by using trypan blue dye exclusion method. Data are mean ± SD of three experiments (*$p < 0.005$). Right panel; PBMCs from patients with ATL (ATL 13–17) and those from healthy donors (Normal 1 and 2) were treated with different amounts of AKI (0, 2.5 or 10 μM) for 48 hr and cell viability was measured by WST-8 assay. (*b*) Jurkat and HUT-102 cells were treated with [AKI (+)] or without [AKI (−)] Aurora kinase inhibitor (10 μM) for the indicated time periods. Cell cycle was analyzed by flow cytometry. (*c*) HTLV-1-infected (SLB-1 and HUT-102) and uninfected (Jurkat and MOLT-4) T-cell lines were treated with AKI (10 μM) for 24 hr. Cells were harvested and stained with Annexin V. The percentage of apoptotic cells was determined by flow cytometry. Data are mean ± SD of three separate transfections. (*$p < 0.005$). (*d*) Jurkat, MOLT-4 and HUT-102 cells were treated with AKI (10 μM) for 24 hr. Western blotting was performed with cleaved PARP antibody. Actin was shown as a loading control. Representative results of three experiments with similar findings.

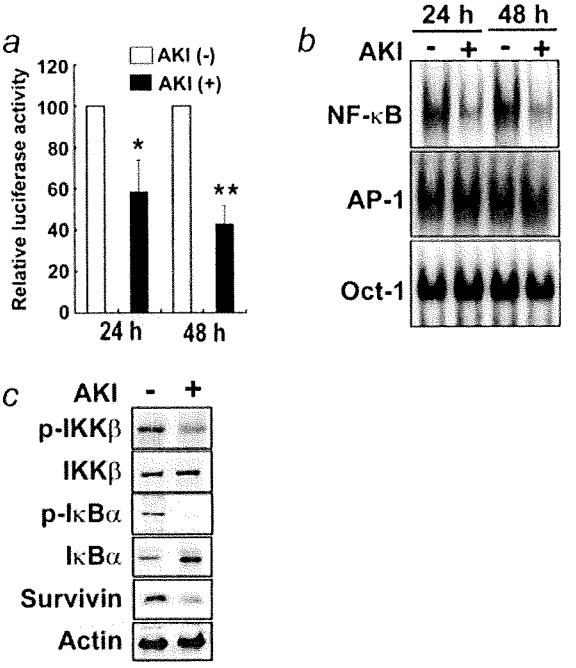

FIGURE 5 – Aurora kinase inhibitor suppresses NF-κB activity in an HTLV-1-infected T-cell line. (*a*) HUT-102 cells were transfected with κB-LUC. At 24-hr after transfection, cells were treated with or without 10 μM AKI for 24 or 48 hr. Luciferase activity was expressed relative to the basal level measurement in cells transfected with the reporter plasmid without further treatment, which was defined as 100. Data are mean ± SD of three separate transfections. (*$p < 0.05$, **$p < 0.005$). (*b*) HUT-102 cells were treated with (+) or without (−) 10 μM AKI for 24 or 48 hr. Nuclear protein was extracted from the cells and NF-κB and AP-1-DNA binding activity was determined by EMSA by using oligonucleotide probes. An oligonucleotide probe for Oct-1 was used as a control. (*c*) HUT-102 cells were treated with 10 μM AKI for 24 hr. Western blotting was performed with the indicated antibodies. Data in (*b*) and (*c*) are representative results of three experiments with similar findings.

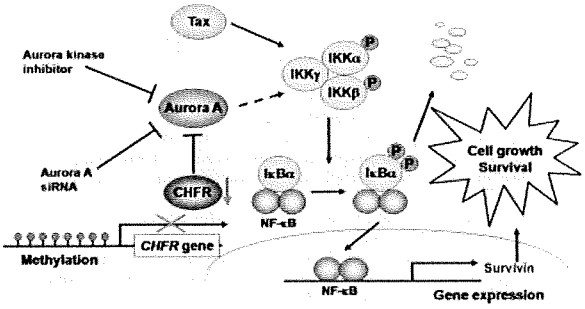

FIGURE 6 – Schematic representation of the effects of Aurora A on cell growth and survival. Loss of CHFR expression by aberrant methylation stabilizes Aurora A protein. Aurora A enhances Tax-induced IKK complex activity and expression of NF-κB regulated antiapoptotic genes such as survivin, leading to enhanced cell growth and survival of HTLV-1-infected T cells.

A and B proteins in a variety of human leukemia cell lines, including 4 HTLV-1-infected T-cell lines, as well as in freshly isolated leukemia cells from individuals with ATL compared with PBMCs from healthy volunteers. Our results also showed that Aurora A mRNA expression level was similar in ATL cells and normal PBMCs, suggesting that overexpression of Aurora A was not due to upregulation of transcription of *Aurora A* gene but rather due to stabilization of this protein. These results are different to those reported by Ikezoe *et al.*[43] who demonstrated different expression levels of Aurora A and B mRNA in ATL cells and normal PBMCs. RT-PCR experiments in our study were not quantitative and the number of primary ATL samples was limited in both the study of Ikezoe *et al.* and the present study, making it difficult to draw firm conclusions on the importance of this finding, emphasizing the need for further studies to establish the true status of Aurora A mRNA level.

CHFR mRNA expression was decreased in HTLV-1-infected T-cell lines than in uninfected T-cell lines. The expressions of CHFR mRNA were invert associated with Aurora A protein levels. CHFR mRNA was also decreased in primary ATL cells than in normal PBMCs. Unfortunately enough ATL patients' samples were not available to analyze both expression of CHFR mRNA

and Aurora A protein in parallel. 5-aza-dC treatment restored CHFR mRNA levels in both HTLV-1-infected T-cell lines and ATL cells. We found HTLV-1-infected T-cell lines that harbored densely methylated CpG sites. Methylation in a gene promoter region generally correlates with a silenced gene. Methylated state in the gene promoter may change the chromatin structure to suppress accessibility of transcription factors to the promoter region. Our findings are indicating that aberrant methylation of the 5′ CpG island of *CHFR* gene is responsible for decreased levels of CHFR mRNA in HTLV-1-infected T-cell lines and ATL cells. Transient expression of CHFR in HUT-102 cells reduced Aurora A protein, consisting with previous study.[9]

Both Tax-dependent and -independent activation of the NF-κB pathway are crucial for cell proliferation, protection against apoptosis and drug resistance in ATL.[19] Tax activates NF-κB by stimulating the activity of IKK complex, which in turn leads to phosphorylation and degradation of IκBα.[19] The present study demonstrated that Aurora A enhanced Tax-induced NF-κB activity but Aurora A mutant lacking kinase activity did not, indicating that the kinase activity of Aurora A is necessary to enhance NF-κB signaling. We reported previously that Bay 11-7082, an NF-κB inhibitor, blocked constitutive NF-κB activation and induced apoptosis of HTLV-1-infected T-cells.[40] Here, we found that treatment with Aurora kinase inhibitor suppressed constitutively activated NF-κB signaling in HTLV-1-infected T-cell lines. Knockdown of Aurora A reduced phosphorylation of IKKβ, but not IKKα or IKKγ (data not shown). Similar to knockdown of Aurora A, Aurora kinase inhibitor reduced phosphorylation of IKKβ, resulting in reduced phosphorylation of IκBα and stabilization of this protein. Treatment with Aurora kinase inhibitor downregulated survivin, an inhibitor of apoptosis family proteins, in HTLV-1-infected T-cell line. Previous studies from our laboratories and those of others showed high expression levels of survivin in freshly obtained leukemic cells from patients with ATL and HTLV-1-infected T-cell lines,[44,45] and that such expression was upregulated through NF-κB pathway in HTLV-1-infected T cells.[42] These results suggest that the apoptotic effect of Aurora kinase inhibitor on HTLV-1-infected T-cell lines is probably mediated through suppression of survivin expression, which is in turn mediated by inhibition of NF-κB.

Although, Aurora kinase inhibitor reduced the cell viability of HTLV-1-infected T-cell lines and ATL cells dramatically, the effects of Aurora kinase inhibitor on NF-κB reporter activity was moderate. Moderate effects of Aurora kinase inhibitor on NF-κB reporter activity cannot explain the significant effects on growth and survival of these cells. There might be other mechanisms which are more important for suppression for the growth and survival of HTLV-1-infected T-cells. Aurora kinase inhibitor which we used for this study was not Aurora A specific. Further studies by using Aurora A specific inhibitor are necessary to find out the specific role of Aurora A on the growth and survival of HTLV-1-infected T-cells.

Recent studies[26,27] have shown that Aurora A activates NF-κB signaling pathway, consistent with the present results. Aurora A induced phosphorylation of IκBα, thereby mediating its degradation and loss of IκBα, which leads to activation of NF-κB target gene transcription.[26] In this regard, inhibition of Aurora kinases was reported to downregulate NF-κB activity and to enhance the efficacy of cytotoxic drugs on lung and ovarian cancer cell lines.[27] However direct target of Aurora A have not been identified in NF-κB signaling molecules. In this study, we found that Aurora A activated Tax-induced NF-κB reporter activity, however without Tax it could not activate NF-κB reporter (Fig. 3*c* right panel), indicating that Aurora A activation of NF-κB is not dominant over Tax. Whether Aurora A activates NF-κB activity by direct phosphorylation of IKKβ or by synergistic way with Tax in HTLV-1-infected T cells requires further investigation.

In conclusion, our results indicated that loss of CHFR expression by aberrant methylation of promoter resulted in stabilization of Aurora A protein. Aurora A enhanced Tax-induced IKK complex activity and expression of NF-κB-regulated antiapoptotic genes such as survivin, leading to enhanced growth and survival of HTLV-1-infected T cells (Fig. 6). The present findings suggested that overexpression of Aurora A might contribute to malignant growth and survival of HTLV-1-infected T cells, making this molecule a potentially suitable target for future therapies for ATL.

Acknowledgements

The authors thank the Fujisaki Cell Center, Hayashibara Biomedical Laboratories (Okayama, Japan) for providing HUT-102 cell line, Dr. J. Fujisawa for providing reporter plasmid κB-LUC and Dr. K. Matsumoto for providing Tax expression plasmid. They also acknowledge all members of their laboratories for the helpful comments and collaborations.

References

1. Giet R, Prigent C. Aurora/Ipl1p-related kinases, a new oncogenic family of mitotic serine-threonine kinases. J Cell Sci 1999;112:3591–601.
2. Andrews PD. Aurora kinases: shining lights on the therapeutic horizon? Oncogene 2005;24:5005–15.
3. Zhou H, Kuang J, Zhong L, Kuo WL, Gray JW, Sahin A, Brinkley BR, Sen S. Tumour amplified kinase STK15/BTAK induces centrosome amplification, aneuploidy and transformation. Nat Genet 1998; 20:189–93.
4. Marumoto T, Zhang D, Saya H. Aurora-A—a guardian of poles. Nat Rev Cancer 2005;5:42–50.
5. Anand S, Penrhyn-Lowe S, Venkitaraman AR. AURORA-A amplification overrides the mitotic spindle assembly checkpoint, inducing resistance to Taxol. Cancer Cell 2003;3:51–62.
6. Warner SL, Bearss DJ, Han H, Von Hoff DD. Targeting Aurora-2 kinase in cancer. Mol Cancer Ther 2003;2:589–95.
7. Mountzios G, Terpos E, Dimopoulos MA. Aurora kinases as targets for cancer therapy. Cancer Treat Rev 2008;34:175–82.
8. Garber K. Divide and Conquer: new generation of drugs targets mitosis. J Natl Cancer Inst 2005;97:874–6.
9. Yu X, Minter-Dykhouse K, Malureanu L, Zhao WM, Zhang D, Merkle CJ, Ward IM, Saya H, Fang G, van Deursen J, Chen J. Chfr is required for tumor suppression and Aurora A regulation. Nat Genet 2005;37:401–6.
10. Scolnick DM, Halazonetis TD. Chfr defines a mitotic stress checkpoint that delays entry into metaphase. Nature 2000;406:430–5.
11. Toyota M, Sasaki Y, Satoh A, Ogi K, Kikuchi T, Suzuki H, Mita H, Tanaka N, Itoh F, Issa JP, Jair KW, Schuebel KE, et al. Epigenetic inactivation of CHFR in human tumors. Proc Natl Acad Sci USA 2003;100:7818–23.
12. Poiesz BJ, Ruscetti FW, Gazdar AF, Bunn PA, Minna JD, Gallo RC. Detection and isolation of type C retrovirus particles from fresh and cultured lymphocytes of a patient with cutaneous T-cell lymphoma. Proc Natl Acad Sci USA 1980;77:7415–9.
13. Hinuma Y, Nagata K, Hanaoka M, Nakai M, Matsumoto T, Kinoshita KI, Shirakawa S, Miyoshi I. Adult T-cell leukemia: antigen in an ATL cell line and detection of antibodies to the antigen in human sera. Proc Natl Acad Sci USA 1981;78:6476–80.
14. Yoshida M, Miyoshi I, Hinuma Y. Isolation and characterization of retrovirus from cell lines of human adult T-cell leukemia and its implication in the disease. Proc Natl Acad Sci USA 1982;79: 2031–5.
15. Tajima K. The 4th nation-wide study of adult T-cell leukemia/lymphoma (ATL) in Japan: estimates of risk of ATL and its geographical and clinical features. The. T- and B-cell Malignancy Study Group. Int J Cancer 1990;45:237–43.
16. Yamada Y, Tomonaga M, Fukuda H, Hanada S, Utsunomiya A, Tara M, Sano M, Ikeda S, Takatsuki K, Kozuru M, Araki K, Kawano F, et al. A new G-CSF-supported combination chemotherapy, LSG15, for adult. T-cell leukaemia-lymphoma: Japan Clinical Oncology Group Study 9303. Br J Haematol 2001;113:375–82.
17. Gill PS, Harrington W, Kaplan MH, Ribeiro RC, Bennett JM, Liebman HA, Bernstein-Singer M, Espina BM, Cabral L, Allen S, Kornblau S, Pike MC, et al. Treatment of adult T-cell leukemia-lymphoma with a combination of interferon α and zidovudine. N Engl J Med 1995;332:1744–8.

18. Grassmann R, Aboud M, Jeang KT. Molecular mechanisms of cellular transformation by HTLV-1 Tax. Oncogene 2005;24:5976–85.
19. Sun SC, Yamaoka S. Activation of NF-κB by HTLV-I and implications for cell transformation. Oncogene 2005;24:5952–64.
20. Karin M. The beginning of the end: IκB kinase (IKK) and NF-κB activation. J Biol Chem 1999;274:27339–42.
21. Karin M, Ben-Neriah Y. Phosphorylation meets ubiquitination: the control of NF-κB activity. Annu Rev Immunol 2000;18:621–63.
22. Marriott SJ, Semmes OJ. Impact of HTLV-I Tax on cell cycle progression and the cellular DNA damage repair response. Oncogene 2005;24:5986–95.
23. Ohshima K, Haraoka S, Yoshioka S, Hamasaki M, Fujiki T, Suzumiya J, Kawasaki C, Kanda M, Kikuchi M. Mutation analysis of mitotic checkpoint genes (hBUB1 and hBUBR1) and microsatellite instability in adult T-cell leukemia/lymphoma. Cancer lett 2000;158:141–50.
24. Nitta T, Kanai M, Sugihara E, Tanaka M, Sun B, Nagasawa T, Sonoda S, Saya H, Miwa M. Centrosome amplification in adult T-cell leukemia and human T-cell leukemia virus type 1 Tax-induced human T cells. Cancer Sci 2006;97:836–41.
25. Afonso P, Zamborlini A, Saib A, Mahieux R. Centrosome and retroviruses: the dangerous liaisons. Retrovirology 2007;4:27.
26. Briassouli P, Chan F, Savage K, Reis-Filho S, Linardopoulos S. Aurora-A regulation of nuclear factor-κB signaling by phosphorylation of IκBα. Cancer Res 2007;67:1689–95.
27. Sun C, Chan F, Briassouli P, Linardopoulos S. Aurora kinase inhibition downregulates NF-κB and sensitises tumour cells to chemotherapeutic agents. Biochem Biophys Res Commun 2007;352:220–5.
28. Tanaka Y, Yoshida A, Takayama Y, Tsujimoto H, Tsujimoto A, Hayami M, Tozawa H. Heterogeneity of antigen molecules recognized by anti-tax1 monoclonal antibody Lt-4 in cell lines bearing human T cell leukemia virus type I and related retroviruses. Jpn J Cancer Res 1990; 81:225–31.
29. Miyoshi I, Kubonishi I, Yoshimoto S, Akagi T, Ohtsuki Y, Shiraishi Y, Nagata K, Hinuma Y. Type C virus particles in a cord T-cell line derived by co-cultivating normal human cord leukocytes and human leukaemic T cells. Nature 1981;294:770–1.
30. Yamamoto N, Okada M, Koyanagi Y, Kannagi M, Hinuma Y. Transformation of human leukocytes by cocultivation with an adult T cell leukemia virus producer cell line. Science 1982;217:737–9.
31. Koeffler HP, Chen IS, Golde DW. Characterization of a novel HTLV-infected cell line. Blood 1984;64:482–90.
32. Tomita M, Choe J, Tsukazaki T, Mori N. The Kaposi's sarcoma-associated herpesvirus K-bZIP protein represses transforming growth factor β signaling through interaction with CREB-binding protein. Oncogene 2004;23:8272–81.
33. Matsumoto K, Shibata H, Fujisawa JI, Inoue H, Hakura A, Tsukahara T, Fujii M. Human T-cell leukemia virus type 1 Tax protein transforms rat fibroblasts via two distinct pathways. J Virol 1997;71:4445–51.
34. Hirota T, Kunitoku N, Sasayama T, Marumoto T, Zhang D, Nitta M, Hatakeyama K, Saya H. Aurora-A and an interacting activator, the LIM protein Ajuba, are required for mitotic commitment in human cells. Cell 2003;114:585–98.
35. Ishiyama M, Tominaga H, Shiga M, Sasamoto K, Ohkura Y, Ueno K. A combined assay of cell viability and in vitro cytotoxicity with a highly water-soluble tetrazolium salt, neutral red and crystal violet. Biol Pharm Bull 1996;19:1518–20.
36. Mori N, Fujii M, Ikeda S, Yamada Y, Tomonaga M, Ballard DW, Yamamoto N. Constitutive activation of NF-κB in primary adult T-cell leukemia cells. Blood 1999;93:2360–8.
37. Susan JC, Harrison J, Paul CL, Frommer M. High sensitivity mapping of methylated cytosines. Nucleic Acids Res 1994;22:2990–7.
38. Xiong Z, Laird PW. COBRA: a sensitive and quantitative DNA methylation assay. Nucleic Acids Res 1997;25:2532–4.
39. Kimura M, Kotani S, Hattori T, Sumi N, Yoshioka T, Todokoro K, Okano Y. Cell cycle-dependent expression and spindle pole localization of a novel human protein kinase, Aik, related to Aurora of drosophila and yeast Ipl1. J Biol Chem 1997;272:13766–71.
40. Mori N, Yamada Y, Ikeda S, Yamasaki Y, Tsukasaki K, Tanaka Y, Tomonaga M, Yamamoto N, Fujii M. Bay 11-7082 inhibits transcription factor NF-κB and induces apoptosis of HTLV-I-infected T-cell lines and primary adult T-cell leukemia cells. Blood 2002;100:1828–34.
41. Mortlock AA, Keen NJ, Jung FH, Heron NM, Foote KM, Wilkinson RW, Green S. Progress in the development of selective inhibitors of aurora kinases. Curr Top Med Chem 2005;5:807–21.
42. Kawakami H, Tomita M, Matsuda T, Ohta T, Tanaka Y, Fujii M, Hatano M, Tokuhisa T, Mori N. Transcriptional activation of survivin through the NF-κB pathway by human T-cell leukemia virus type I tax. Int J Cancer 2005;115:967–74.
43. Ikezoe T, Yang J, Nishioka C, Tasaka T, Taniguchi A, Kuwayama Y, Komatsu N, Bandobashi K, Togitani K, Koeffler HP, Taguchi H. A novel treatment strategy targeting Aurora kinases in acute myelogenous leukemia. Mol Cancer Ther 2007;6:1851–7.
44. Kamihira S, Yamada Y, Hirakata Y, Tomonaga M, Sugahara K, Hayashi T, Dateki N, Harasawa H, Nakayama K. Aberrant expression of caspase cascade regulatory genes in adult T-cell leukaemia: survivin is an important determinant for prognosis. Br J Haematol 2001;114:63–9.
45. Mori N, Yamada Y, Hata T, Ikeda S, Yamasaki Y, Tomonaga M, Yamamoto N. Expression of survivin in HTLV-I-infected T-cell lines and primary ATL cells. Biochem Biophys Res Commun 2001;282: 1110–3.

Epigenetic Profiles Distinguish Malignant Pleural Mesothelioma from Lung Adenocarcinoma

Yasuhiro Goto,[1] Keiko Shinjo,[1,3] Yutaka Kondo,[1] Lanlan Shen,[7] Minoru Toyota,[8] Hiromu Suzuki,[9] Wentao Gao,[10] Byonggu An,[1] Makiko Fujii,[1] Hideki Murakami,[1] Hirotaka Osada,[1,3] Tetsuo Taniguchi,[5] Noriyasu Usami,[5] Masashi Kondo,[4] Yoshinori Hasegawa,[4] Kaoru Shimokata,[11] Keitaro Matsuo,[2] Toyoaki Hida,[6] Nobukazu Fujimoto,[12] Takumi Kishimoto,[12] Jean-Pierre J. Issa,[7] and Yoshitaka Sekido[1,3]

Divisions of [1]Molecular Oncology and [2]Epidemiology and Prevention, Aichi Cancer Center Research Institute; Departments of [3]Cancer Genetics and [4]Respiratory Medicine and [5]Division of General Thoracic Surgery, Nagoya University Graduate School of Medicine; [6]Department of Thoracic Oncology, Aichi Cancer Center Hospital, Nagoya, Japan; [7]Department of Leukemia, The University of Texas M. D. Anderson Cancer Center, Houston, Texas; [8]Department of Biochemistry and [9]First Department of Internal Medicine, Sapporo Medical University, Sapporo, Japan; [10]Department of General Surgery, First Affiliated Hospital of Nanjing Medical University, Nanjing, China; [11]Department of Biomedical Sciences, Chubu University, Kasugai, Japan; and [12]Department of Respiratory Medicine, Okayama Rosai Hospital, Okayama, Japan

Abstract

Malignant pleural mesothelioma (MPM) is a fatal thoracic malignancy, the epigenetics of which are poorly defined. We performed high-throughput methylation analysis covering 6,157 CpG islands in 20 MPMs and 20 lung adenocarcinomas. Newly identified genes were further analyzed in 50 MPMs and 56 adenocarcinomas via quantitative methylation-specific PCR. Targets of histone H3 lysine 27 trimethylation (H3K27me3) and genetic alterations were also assessed in MPM cells by chromatin immunoprecipitation arrays and comparative genomic hybridization arrays. An average of 387 genes (6.3%) and 544 genes (8.8%) were hypermethylated in MPM and adenocarcinoma, respectively. Hierarchical cluster analysis showed that the two malignancies have characteristic DNA methylation patterns, likely a result of different pathologic processes. In MPM, a separate subset of genes was silenced by H3K27me3 and could be reactivated by treatment with a histone deacetylase inhibitor alone. Integrated analysis of these epigenetic and genetic alterations revealed that only 11% of heterozygously deleted genes were affected by DNA methylation and/or H3K27me3 in MPMs. Among the DNA hypermethylated genes, three (*TMEM30B, KAZALD1*, and *MAPK13*) were specifically methylated only in MPM and could serve as potential diagnostic markers. Interestingly, a subset of MPM cases (4 cases, 20%) had very low levels of DNA methylation and substantially longer survival, suggesting that the epigenetic alterations are one mechanism affecting progression of this disease. Our findings show a characteristic epigenetic profile of MPM and uncover multiple distinct epigenetic abnormalities that lead to the silencing of tumor suppressor genes in MPM and could serve as diagnostic or prognostic targets. [Cancer Res 2009;69(23):9073–82]

Introduction

Malignant pleural mesothelioma (MPM) is an aggressive tumor that has been associated with asbestos exposure (1). Approximately 10,000 to 15,000 patients worldwide are newly diagnosed with MPM annually, and the number of patients is projected to increase over the next two decades in Asia and the United States (1, 2). Although the inhalation of asbestos is a well-known risk factor, the lack of clinical symptoms in the early stages of MPM as well as of useful diagnostic markers makes early diagnosis virtually impossible. In addition to these difficulties, the relative ineffectiveness of available therapies also contributes to the death of MPM patients shortly after diagnosis (1, 3). Therefore, further molecular analysis of MPM is urgently needed to identify effective markers that could be applied to blood or pleural fluid for an early valid diagnosis.

The central mechanisms underlying MPM formation are still unclear. Several genetic abnormalities seem to be involved in MPM, such as a loss of the *p16* locus or mutations in the *NF2* gene (4–6). However, recent whole-transcriptome sequencing approaches as well as comparative genomic hybridization analyses have revealed relatively few genetic mutations in MPM, about six genes per individual MPM (7, 8). The low frequency of genetic abnormalities raises the question of whether alternative mechanisms might also be contributing to the inactivation of genes, leading to tumor formation.

Dysregulation of epigenetic transcriptional control, particularly aberrant promoter DNA methylation and histone modifications, is a fundamental feature of human malignancies (9). The relationship between promoter DNA hypermethylation and inflammation has been documented in many types of cancers, including MPM (10). It could be that asbestos exposure contributes to MPM formation through this relationship (11–14), because it is known that asbestos induces continuous inflammation instead of directly transforming primary human mesothelial cells in tissue culture (15–17). In addition, recent cumulative studies of aberrant DNA methylation in human cancers showed high rates of aberrant promoter methylation in a subset of cancers, termed the CpG island methylator phenotype, which may also be contributing to MPM formation (18). However, there is currently limited information available regarding the DNA methylation status of MPM.

In addition to DNA methylation, a dysregulation of histone H3 lysine 27 trimethylation (H3K27me3) is known to be involved in several human malignancies (19). Enhancer of zeste 2, a polycomb

Note: Supplementary data for this article are available at Cancer Research Online (http://cancerres.aacrjournals.org/).

Y. Goto and K. Shinjo contributed equally to this work.

Requests for reprints: Yutaka Kondo, Division of Molecular Oncology, Aichi Cancer Center Research Institute, 1-1 Kanokoden, Chikusa-ku, Nagoya 464-8681, Japan. Phone: 81-52-764-2993; Fax: 81-52-764-2993; E-mail: ykondo@aichi-cc.jp.

doi:10.1158/0008-5472.CAN-09-1595

group protein part of polycomb repressor complex 2, has histone methyltransferase activity with substrate specificity for H3K27. Because polycomb group–mediated gene silencing is initiated by the histone deacetylase (HDAC) activity of polycomb repressor complex 2, inhibition of HDAC can efficiently reactivate the H3K27me3 target genes (20, 21). However, this epigenetic event has not been studied in MPM.

To investigate aberrant epigenetic events in MPM, we performed global screening for genes with aberrant DNA hypermethylation using the methylated CpG island amplification microarray (MCAM), which provides reproducible results with a high validation rate and successfully detects genes methylated in normal as well as in cancerous tissues (22, 23). We also conducted combined analysis of MCAM, chromatin immunoprecipitation-microarrays, and array comparative genomic hybridization to show the relationship between these epigenetic and genetic abnormalities in MPMs. Our comprehensive analysis revealed that multiple epigenetic abnormalities play important roles in MPM carcinogenesis and may be valid therapeutic targets.

Materials and Methods

Cell lines. Two MPM cell lines [ACC-MESO-1 (MESO1) and Y-MESO-8A (MESO8)] previously established in our laboratory (24) and one nonmalignant mesothelial cell line (MeT-5A) were used for the study. MeT-5A was purchased from the American Type Culture Collection and cultured according to the instructions (CRL-9444). MESO1 and MESO8 were maintained in RPMI 1640 (Sigma-Aldrich) supplemented with 10% fetal bovine serum (Invitrogen) and antibiotic-antimycotic (Invitrogen) at 37°C in a humidified incubator with 5% CO_2.

Tissue samples. Fifty MPM samples, 56 adenocarcinoma samples, 4 normal mesothelial tissues, and 10 normal lung tissues were obtained from Japanese patients at the Aichi Cancer Center Hospital, Nagoya University Hospital, and the affiliated hospitals. Samples and clinical data were collected after appropriate institutional review board approval was received and written informed consent had been obtained from all patients. We scraped the surface of the resected normal lung from lung cancer cases and obtained normal pleural tissues. Normal lung tissues were obtained from the normal lung of lung cancer cases. Histologic and cytologic examination of both normal mesothelial and lung tissues revealed no remarkable findings as malignant tissues. In these normal tissues, no aberrant methylation was detected in five genes with pyrosequencing analysis (Supplementary Table S1).

DNA preparation. Genomic DNA was extracted using a standard phenol-chloroform method. Fully methylated DNA was prepared by treating genomic DNA with *SssI* methylase (New England Biolabs; ref. 23). Unmethylated DNA was prepared by treating genomic DNA with phi29 DNA polymerase (GenomiPhi DNA Amplification kit; Amersham Biosciences) according to the manufacturer's protocol.

Methylated CpG island amplification-microarray. For MCAM analysis, we analyzed 20 MPMs (average age, 59.1 years; range, 45-78 years) and 20 adenocarcinomas (average age, 62.8 years; range, 44-76 years). A detailed protocol of MCAM has been described previously (22, 23). We used a human custom promoter array (G4497A; Agilent Technologies) containing 15,134 probes corresponding to 6,157 unique genes (23).

Hierarchical clustering analysis. Cluster analysis was done using an agglomerative hierarchical clustering algorithm (23, 25). For specimen clustering, pairwise similarity measures among specimens were calculated using Cluster 3.0 software[13] or Minitab 15 statistical software[14] based on the DNA methylation intensity measurements across all genes.

[13] http://rana.lbl.gov/EisenSoftware.htm
[14] http://www.minitab.com

Methylation analysis. We performed bisulfite treatment as described previously (26, 27). The DNA methylation levels were measured using Pyrosequencing technology. For each assay, the setup included both positive controls (samples after *SssI* treatment) and negative controls (samples after whole-genome amplification using GenomiPhi V2), with mixing experiments to rule out bias, and repeat experiments to assess reproducibility (28). Conventional methylation-specific PCR (MSP) was also carried out for the *transmembrane protein 30B* (*TMEM30B*), *Kazal-type serine protease inhibitor domain 1* (*KAZALD1*), and *mitogen-activated protein kinase 13* (*MAPK13*) genes. PCR products were visualized on 6% polyacrylamide or 3% agarose gels stained with ethidium bromide. MSP products were subsequently confirmed by bisulfite sequencing analysis. Quantitative MSP was also carried out using SYBR Green (Applied Biosystems). In addition to primers designed specifically for the gene of interest, an internal reference primer set designed for *LINE1*, which can amplify *LINE1* loci irrespective of DNA methylation status, was included in the analysis to normalize for input DNA. The percentage methylated reference is calculated by dividing the GENE:LINE1 ratio of the sample by the GENE:LINE1 ratio of the *SssI*-treated methylated DNA and multiplying by 100 (29). To determine the cutoff value for the classification of methylated and unmethylated loci, we compared the percentage methylated reference and the methylation level from pyrosequencing analysis in each gene. The best discrimination cutoff values were 7% for *TMEM30B*, 5% for *KAZALD1*, and 5% for *MAPK13*. Primer sequences and PCR conditions are shown in Supplementary Table S2. All of the primers were designed to examine the methylation status of CpGs within 0.5 kb of the transcription start site.

Trichostatin A and 5-aza-2′-deoxycytidine treatment of cells. Cells were treated with 5-aza-2′-deoxycytidine (5Aza-dC; Sigma-Aldrich) or trichostatin A (MP Biomedicals) as described previously (23).

Chromatin immunoprecipitation-microarrays. Chromatin immunoprecipitation was done based on the previously published methods (21, 30). Trimethylated H3K27-specific samples and the input samples were labeled with Cy5 and Cy3, respectively. Labeled chromatin immunoprecipitation products were hybridized to CpG microarray using the same protocol as MCAM. A Cy5/Cy3 signal in excess of 1.5 was considered as an enrichment of H3K27me3 (Supplementary Table S3).

Quantitative reverse transcription-PCR analyses. Total RNA was isolated using Trizol (Invitrogen). RNA (2 μg) was reverse transcribed with MPMLV (Promega). TaqMan quantitative reverse transcription-PCRs and SYBR Green quantitative reverse transcription-PCRs were carried out in triplicate for the target genes (Applied Biosystems). Primer sequences are shown in Supplementary Table S2.

Statistical analysis. Associations between methylation status and clinicopathologic variables were analyzed by the Mann-Whitney *U* test, Fisher's exact test, Kruskal-Wallis test, or a linear regression model. The Kaplan-Meier method was used to estimate overall survival. The Cox proportional hazards models were used for estimation of hazard ratio. All reported *P* values were two-sided, with $P < 0.05$ considered statistically significant. Calculations were carried out with either StatView software version 5.0 (Abacus Concepts) or Stata version 8 (StataCorp).

Results

DNA methylation profiling by MCAM analysis in MPM and adenocarcinoma. To compare the global DNA methylation profiles of MPM and adenocarcinoma, we analyzed 20 samples of each using MCAM. Technical replications of MCAM were done for six cases of MPM and highly reproducible methylation profiles were obtained among the replicates ($R^2 = 0.93$; Supplementary Fig. S1). A Cy5/Cy3 signal in excess of 2.0 in MCAM was considered methylation-positive in a previous study (23). In the present study, 18 randomly selected genes were subsequently assessed by pyrosequencing analysis in MPM and adenocarcinoma samples. A methylation level >15% was considered methylation-positive (23). A high concordance was observed between the methylation status by

MCAM and pyrosequencing analyses (specificity, 90%; sensitivity, 82%; Supplementary Table S4) as was also shown in previous studies (22, 23). We will hereafter consider a signal ratio >2.0 in MCAM as methylation-positive.

In the cohybridization of MCA products from normal mesothelium DNA and normal lung tissue DNA, a high concordance in the methylation status was observed (R^2 = 0.87; Fig. 1*A*), suggesting that tissue-specific methylation is rare in these two tissues.

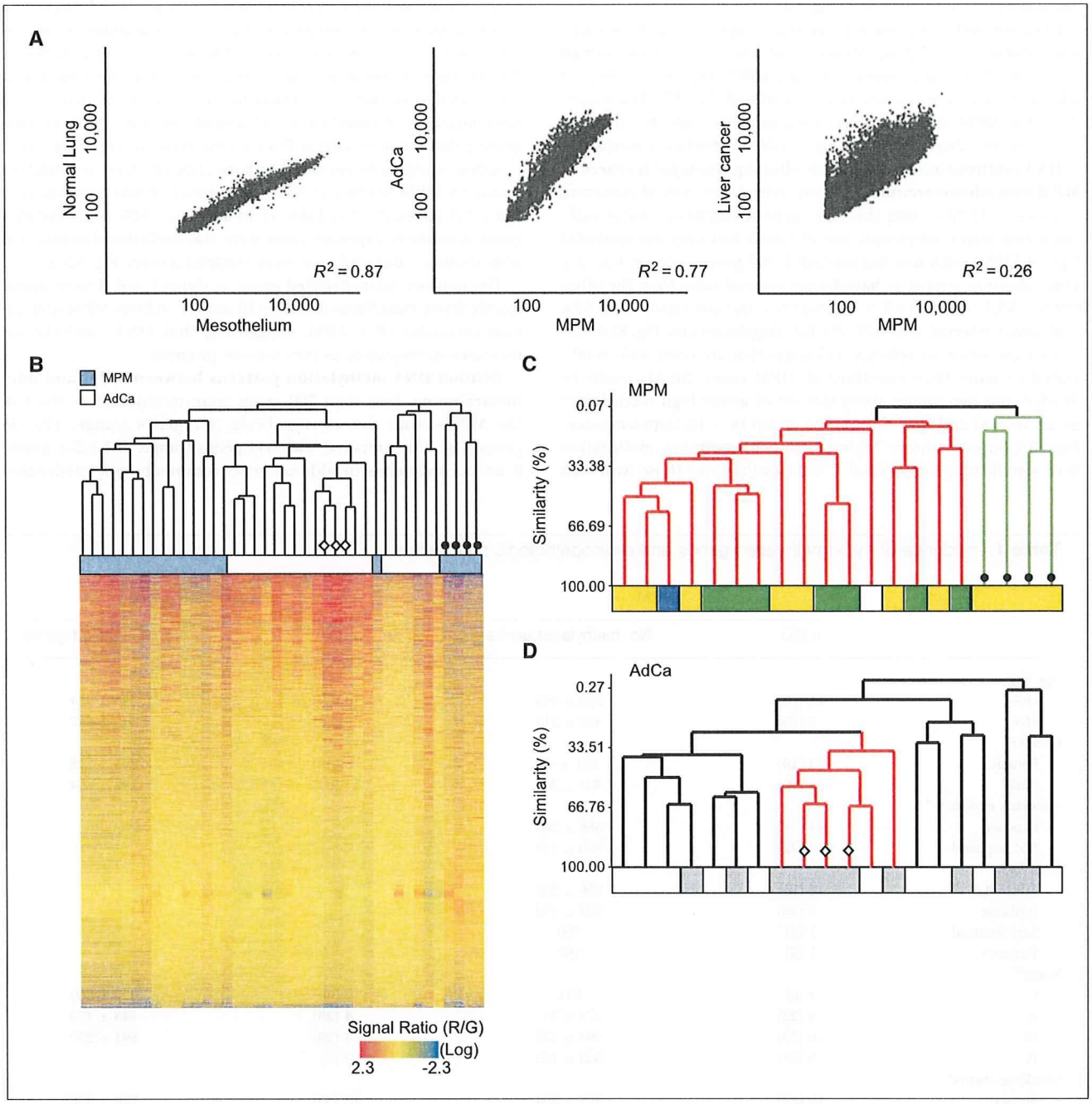

Figure 1. DNA methylation profiling by MCAM analysis. *A,* scatter plot analysis of signal intensity (log scale) between normal mesothelium (mixture of two cases) and normal lung tissue (mixture of four cases; *left*), MPM and adenocarcinoma (*AdCa*; both a mixture of four cases in both tumors; *middle*), and MPM and liver cancer (both a mixture of four cases in both tumors, *right*). The coefficient of determination (R^2) in the linear regression model is indicated in each analysis. *B,* dendrogram and heat-map overview of hierarchical cluster analysis of DNA methylation data from 40 samples (*blue boxes,* MPM; *white boxes,* adenocarcinoma) using all 6,157 genes (*Y axis*). Color corresponds to methylation level as indicated in the $\log_2$-transformed scale bar below the matrix. *Red* and *blue,* high and low levels, respectively; *black circle,* <300 genes methylated in these MPMs; *open diamond,* >950 genes methylated in these adenocarcinomas. *C,* defining subclasses in MPMs using hierarchical clustering. All 6,157 genes were used for the analysis of 20 MPMs. *Y axis,* similarity. Color boxes indicate histologic subtype of MPM. *Yellow, green, blue,* and *white boxes,* epithelial, biphasic, sarcomatoid, and variants, respectively; *black circle,* same MPMs as in *B. D,* subclasses in adenocarcinomas using hierarchical clustering. *Y axis,* similarity. *Gray* and *white boxes,* smokers and nonsmokers, respectively; *open diamond,* same adenocarcinomas as in *B.*

Although ~70% of hypermethylated genes in MPMs were also found to be methylated in adenocarcinoma, a subset of loci were differently methylated in each tumor (R^2 = 0.77; Fig. 1*A*; Supplementary Fig. S2*A*). Interestingly, a larger number of loci were differently methylated in MPM and liver cancer (ref. 23; R^2 = 0.26), suggesting that the methylation profiles of MPM and adenocarcinoma have more in common (Fig. 1*A*).

Unsupervised hierarchical clustering analysis using the methylation status of 6,157 genes showed that adenocarcinomas seemed to be more frequently methylated than MPMs and that a subset of adenocarcinomas was extensively methylated (Fig. 1*B*). The majority of the MPM and adenocarcinoma samples could be classified into distinct subgroups according to DNA methylation status.

DNA methylation status affects clinicopathologic features of MPM and adenocarcinoma. Unsupervised hierarchical clustering analysis of MPMs using the 6,157-gene methylation status indicated two major subgroups, one of which had only the epithelial type of MPMs with less methylation (<300 genes; 4 cases; Fig. 1*C*). This subgroup tended to have longer survival rates than the other (19.5 ± 13.7 versus 14.5 ± 3.3 months; hazard ratio, 0.48; 95% confidence interval, 0.10-2.21; P = 0.3; Supplementary Fig. S3*A*). Interestingly, when we selected 445 genes that are commonly methylated in more than one-third of MPM cases, MPMs could be divided into two groups using this set of genes: high methylation group (n = 8) and low methylation group (n = 10; Supplementary Fig. S3*B*; Supplementary Table S5). Patients with low methylation lived significantly longer (21.6 ± 13.3 months) than those with high methylation (6.8 ± 4.1 months; hazard ratio, 0.16; 95% confidence interval, 0.04-0.63; P < 0.01; Supplementary Fig. S3*C*).

Adenocarcinomas were divided into four subgroups (Fig. 1*D*). One subgroup consisted of six adenocarcinoma samples that had more methylated genes than the other samples (911 ± 220 versus 387 ± 231 genes; P < 0.01) and came mostly from smokers (5 of 6 cases; mean pack-years smoked, 68.6 ± 22.9 years). Smokers had significantly more methylated genes than nonsmokers in adenocarcinoma (728 ± 338 versus 360 ± 206 genes; P = 0.02; Table 1). The majority of methylated genes (82%) in nonsmokers were also methylated in smokers (Supplementary Fig. S2*B*). In contrast, there were numbers of specifically methylated genes in smokers, suggesting that smoking affects DNA methylation in a set of genes.

Asbestos exposure appeared to have little effect on methylation status in MPM (exposure 386 ± 203 genes versus nonexposure 320 ± 118 genes; P = 0.4; Table 1). In addition, >60% of methylated genes in asbestos exposure cases were also methylated in asbestos nonexposure cases and vice versa (Supplementary Fig. S2*C*).

The numbers of methylated genes in stages I and II were significantly fewer than those in stages III and IV in both MPM and adenocarcinoma (P < 0.05), suggesting that DNA methylation increases in frequency as the diseases progress.

Distinct DNA methylation patterns between MPM and adenocarcinoma. Less than 700 genes were methylated in most of the MPMs, with the average being 387 genes (range, 120-755 genes; Fig. 2*A*) compared with 544 genes (range, 133-1,212 genes) in adenocarcinomas. In addition, genes commonly hypermethylated

Table 1. Incidence of hypermethylated genes and clinicopathologic parameters

	MPM		Adenocarcinoma	
	n (%)	No. methylated genes	*n* (%)	No. methylated genes
Age (y)*				
<65	14 (75)	388 ± 193	10 (50)	546 ± 404
≥65	5 (25)	430 ± 212	10 (50)	542 ± 262
Gender				
Female	2 (10)	261 ± 46	8 (40)	395 ± 218
Male	18 (90)	401 ± 202	12 (60)	643 ± 364
Asbestos exposure*				
Exposed	14 (78)	386 ± 203		
Not exposed	4 (22)	320 ± 118		
Histology				
Epithelial	11 (55)	356 ± 208		
Biphasic	7 (35)	403 ± 172		
Sarcomatoid	1 (5)	700		
Variants	1 (5)	297		
Stage*†				
I	1 (6)	211	12 (60)	427 ± 269
II	4 (25)	174 ± 76	4 (20)	748 ± 473
III	6 (38)	394 ± 179	4 (20)	691 ± 259
IV	5 (31)	308 ± 162	0 (0)	
Smoking status*				
Smoker	14 (88)	367 ± 204	10 (50)	728 ± 338‡
Nonsmoker	2 (12)	261	10 (50)	360 ± 206

*Clinical data of some patients were unavailable.
†Number of methylated genes in I and II is significantly smaller than in III and IV in MPMs and adenocarcinomas (P < 0.05).
‡Number of methylated genes in this group is significantly higher (P < 0.05) than in the other group.

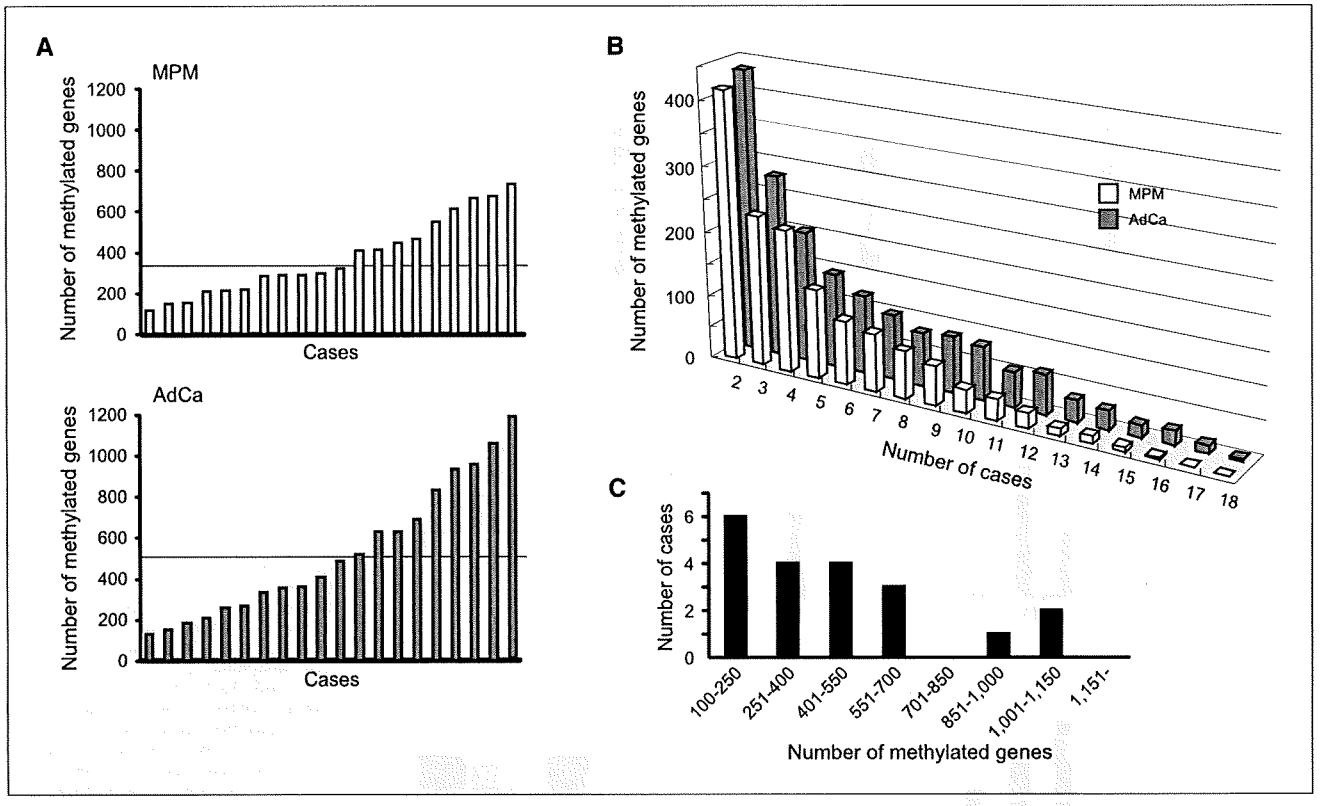

Figure 2. Comparison of distinct DNA methylation patterns between MPM and adenocarcinoma. *A*, number of methylated genes in each case. *Line*, average numbers of methylated genes (387 and 544 genes in MPM and adenocarcinoma, respectively). *B*, number of genes (*Y axis*) that were commonly methylated in *x* number of cases, where *x* is the axis in MPM (*white*) or adenocarcinoma (*gray*). *C*, bimodal distribution of methylated genes out of 1,457 loci in adenocarcinoma. The number of methylated genes (*X axis*) is plotted against the number of cases (*Y axis*).

in >10 MPMs were quite rare (<40 genes), whereas >80 genes were commonly hypermethylated in 10 adenocarcinomas, suggesting that hypermethylated genes vary more in each MPM case ($P < 0.01$; Fig. 2*B*). Notably, analysis of 1,457 genes that were methylated in >2 adenocarcinoma cases showed the bimodal distribution of methylation pattern as shown previously in CpG island methylator phenotype–positive tumor (ref. 31; Fig. 2*C*).

Two epigenetic mechanisms regulating gene expression in MPM cell lines. We next examined the changes in expression of genes identified by MCAM analysis before and after epigenetic treatments (Fig. 3*A*). These genes were methylated to some extent and were silenced in both MPM cell lines, MESO1 and MESO8, in contrast to their high expression levels in normal mesothelial tissue. Each gene in the different cell lines responded differently to the epigenetic treatments. *Ankyrin 1* (*ANK1*) was reactivated by the DNA methyltransferase inhibitor, 5Aza-dC, in a dose-dependent manner but was not reactivated by a HDAC inhibitor trichostatin A alone, which is the typical response to epigenetic treatment in DNA methylation target genes (32). *Progesterone receptor* (*PGR*) was reactivated by both 5Aza-dC and trichostatin A alone regardless of its DNA methylation status. Unexpectedly, the response to trichostatin A treatment in *proenkephalin* (*PENK*) differed between these two cell lines, although the CpG island in both cell lines was densely methylated. These findings, taken together, most likely indicate that another epigenetic mechanism regulates gene expression in MPM cells.

H3K27me3 mediated by polycomb group protein is an alternative silencing mechanism for tumor suppressor genes in human malignancies (19). We examined the H3K27me3 status in the same three genes (Fig. 3*B*). H3K27me3 was enriched in the *PGR* promoter in both cell lines and in the *PENK* promoter in MESO8. No enrichment of H3K27me3 was observed in either the *PENK* promoter in MESO1 or in the *ANK1* promoter in both cell lines that are densely DNA methylated.

Integrated analysis of genetic and epigenetic alterations. To examine H3K27me3 targets and the relation between DNA methylation and H3K27me3 on the CpG promoters in MPM cells, we carried out a chromatin immunoprecipitation-microarray analysis using the same promoter array (Fig. 4*A*). First, we validated the chromatin immunoprecipitation-microarray results by chromatin immunoprecipitation-PCR with randomly selected genes and found good concordance between the two analyses (specificity, 82%; sensitivity, 82%; Supplementary Table S3). We counted the genes that were enriched with H3K27me3 in MESO1 or MESO8 but not enriched in MeT-5A (a nonmalignant mesothelial cell line) and found 113 and 241 target genes in MESO1 and MESO8, respectively (Fig. 4*A*). DNA methylation was more frequently observed than H3K27me3 in the CpG promoters in both cell lines. There was some overlap between DNA-methylated and H3K27me3 target genes; however, the majority of the genes enriched with H3K27me3 revealed no detectable DNA hypermethylation, whereas most genes showing DNA hypermethylation showed no enrichment with H3K27me3. These results suggest that DNA hypermethylation and

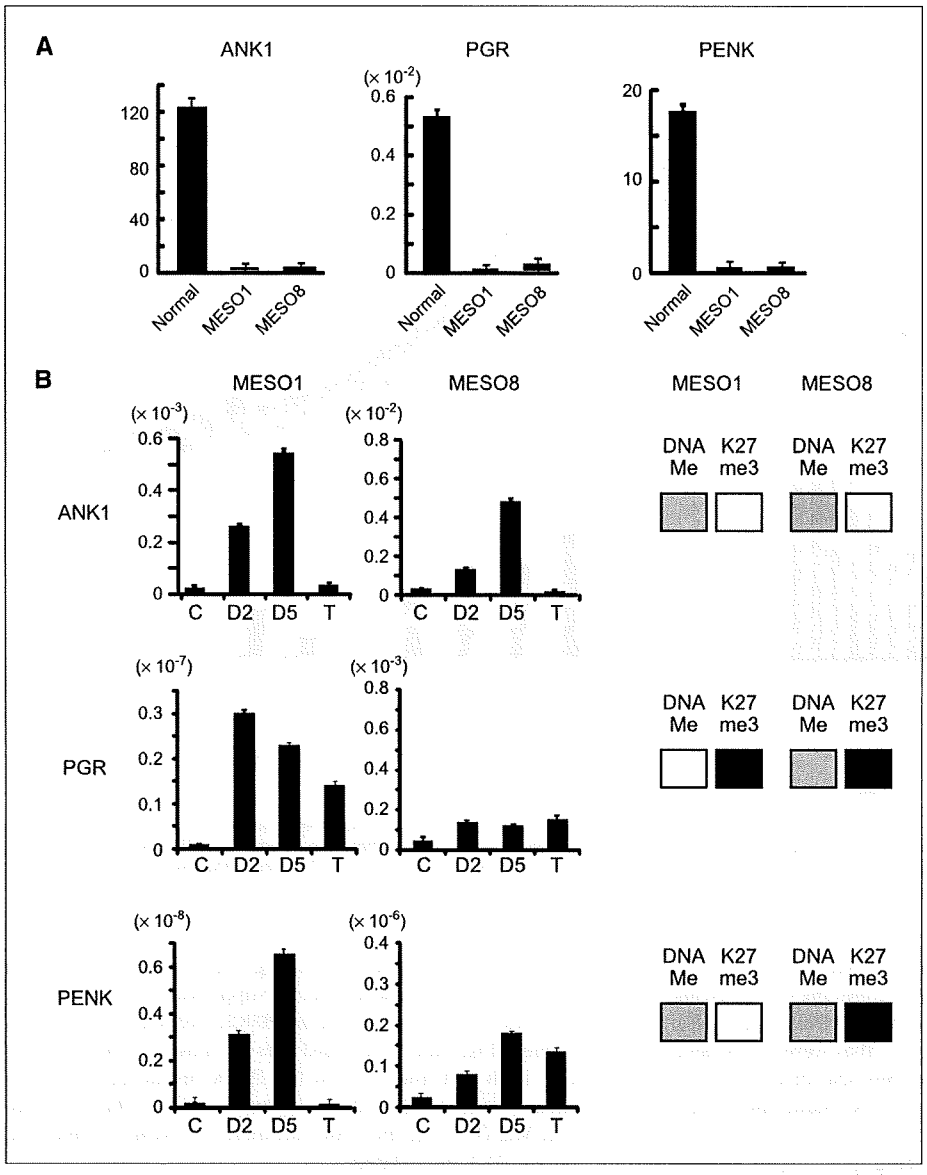

Figure 3. Relationship between gene expression and epigenetic alterations in MPM cell lines. *A*, gene expression was measured by quantitative PCR in normal mesothelial tissue, MESO1, and MESO8. *Y axis*, relative values of mRNA expression for each gene to glyceraldehyde-3-phosphate dehydrogenase. *Bars*, SD from experiments in triplicate. *B*, reactivation of silenced genes by DNA methyltransferase inhibitor (5Aza-dC) or HDAC inhibitor (trichostatin A) in three representative genes. After treatment with either PBS (control; *C*), 2 μmol/L (*D2*) or 5 μmol/L (*D5*) 5Aza-dC, or trichostatin A (*T*), each silenced gene was reactivated. *Y axis*, relative values of mRNA expression for each gene to glyceraldehyde-3-phosphate dehydrogenase. *Right columns*, status of DNA methylation (*DNA Me*) and H3K27me3 (*K27me3*). Regarding levels of DNA methylation in these genes, each gene shows high (*gray*; DNA methylation level >60%) or low (*white*; DNA methylation level <10%) methylation. For H3K27me3, each gene shows enrichment (*black*) or nonenrichment (*white*) of H3K27me3. DNA methylation levels were assayed by pyrosequencing and H3K27me3 status was assayed by chromatin immunoprecipitation-microarray and chromatin immunoprecipitation-PCR.

H3K27me3 may contribute to cancer development through the silencing of specific target genes in MPM cells (Fig. 4*A* and *B*).

We next carried out an integrated genetic and epigenetic analysis using array comparative genomic hybridization data that we have reported previously in the same cell lines (33). A total of 5,746 genes covered by both MCAM and comparative genomic hybridization arrays were analyzed. Genomic deletions were detected in 190 and 565 genes in MESO1 and MESO8, respectively. The majority of those genes showed heterozygous deletions, whereas only 8 and 3 genes showed homozygous deletions in MESO1 and MESO8, respectively (Fig. 4*B*). Twenty-one of 190 (11%, MESO1) and 63 of 565 (11%, MESO8) deleted genes were also affected by DNA methylation or H3K27me3, most of which were affected by heterozygous deletions and DNA methylation. Interestingly, all these three events were observed in one gene in MESO8, *A-kinase anchor protein 12* (*AKAP12*), which has been reported as a tumor suppressor gene and a target of DNA methylation in childhood myeloid malignancies (34). Representative analyses of chromosomes 9 and 10 where two important tumor suppressor genes, *CDKN2A* and *PTEN*, were homozygously deleted, showed that genetic deletion is rare. It was also found that genetic deletion, DNA methylation, and H3K27me3 do not frequently overlap on the same loci in these chromosomes (Fig. 4*C*).

Identification of MPM-specific methylation markers. DNA methylation has been proposed as a powerful potential marker for cancer diagnosis (35). To identify specific methylation markers for MPM, we first selected 8 genes from the MCAM analysis, which were methylation-positive (Cy5/Cy3 > 2.0) in at least four MPMs and methylation-negative in all of the adenocarcinomas (Fig. 5*A*). We validated the genes by MSP and found that three of them, *TMEM30B, KAZALD1*, and *MAPK13*, were the best specific methylation markers for MPM (Fig. 5*B* and *C*). In the same set of MPMs analyzed by MCAM, DNA methylation was detected by MSP analysis in 11 (58%), 8 (42%), and 2 (11%) cases of 19 in the *TMEM30B, KAZALD1*, and *MAPK13* genes, respectively.

To confirm whether these methylation markers might prove valid in another group of MPM patients, we obtained an additional 31 MPM samples from a different institution. Altogether, the methylation status of these three genes was analyzed in 50 MPMs by quantitative MSP (Fig. 5*D*). DNA methylation occurred in 19 cases (38%) in *TMEM30B*, 24 (48%) in *KAZALD1*, and 19 (38%) in *MAPK13*. In contrast, no substantial DNA methylation was detected in those three genes in 56 adenocarcinomas (Fig. 5*C* and *D*). The sensitivity and specificity of hypermethylation in at least one of the above three genes for a differential diagnosis of MPM from adenocarcinoma were found to be 72% and 100%, respectively. Kaplan-Meier survival analysis on methylation status of these three MPM-specific methylation genes revealed that MPM patients with no methylation tended to have prolonged survival (n = 11; 17.0 ± 13.9 months) compared with those with at least one gene methylated (n = 34; 12.1 ± 7.8 months; hazard ratio, 0.58; 95% confidence interval = 0.26-1.28; P = 0.17; Supplementary Fig. S3*D*).

Discussion

In this study, we analyzed and compared the DNA methylation status of MPM and adenocarcinoma to highlight the methylation profile of MPM. Although normal mesothelium and lung tissue develop from different germ layers (mesoderm and endoderm, respectively), their hypermethylation profiles are very similar (R^2 = 0.87), indicating that tissue-specific methylation differences in these two normal tissues are infrequent. Previous genome-wide methylation analyses of a variety of normal tissues have consistently shown that tissue-specific methylation is quite rare, thus validating our findings (22, 36, 37). By contrast, the differences in hypermethylated genes between MPM and adenocarcinoma were more numerous than in normal tissues, which might be a result of different pathologic processes in the two malignancies.

A previous study of the methylation status of seven loci showed that methylation is less prevalent in MPM than in adenocarcinoma (11). Our own global DNA methylation analysis revealed that hypermethylated genes are less frequent and more varied overall in MPM than in adenocarcinoma. Fewer than 700 genes were methylated in most of the MPMs (average hypermethylated genes, 387 ± 196 genes). This contrasted with a subset of adenocarcinoma samples, all of them from smokers (mean pack-years smoked, 67.3 ± 14.2 years) that were extensively methylated (>950 genes). In adenocarcinoma, smoking seems to be a mechanism driving tumors into distinct epigenetic subclasses. It has been suggested that certain adenocarcinomas can be predisposed to hypermethylation and a phenotype known as CpG island methylator phenotype

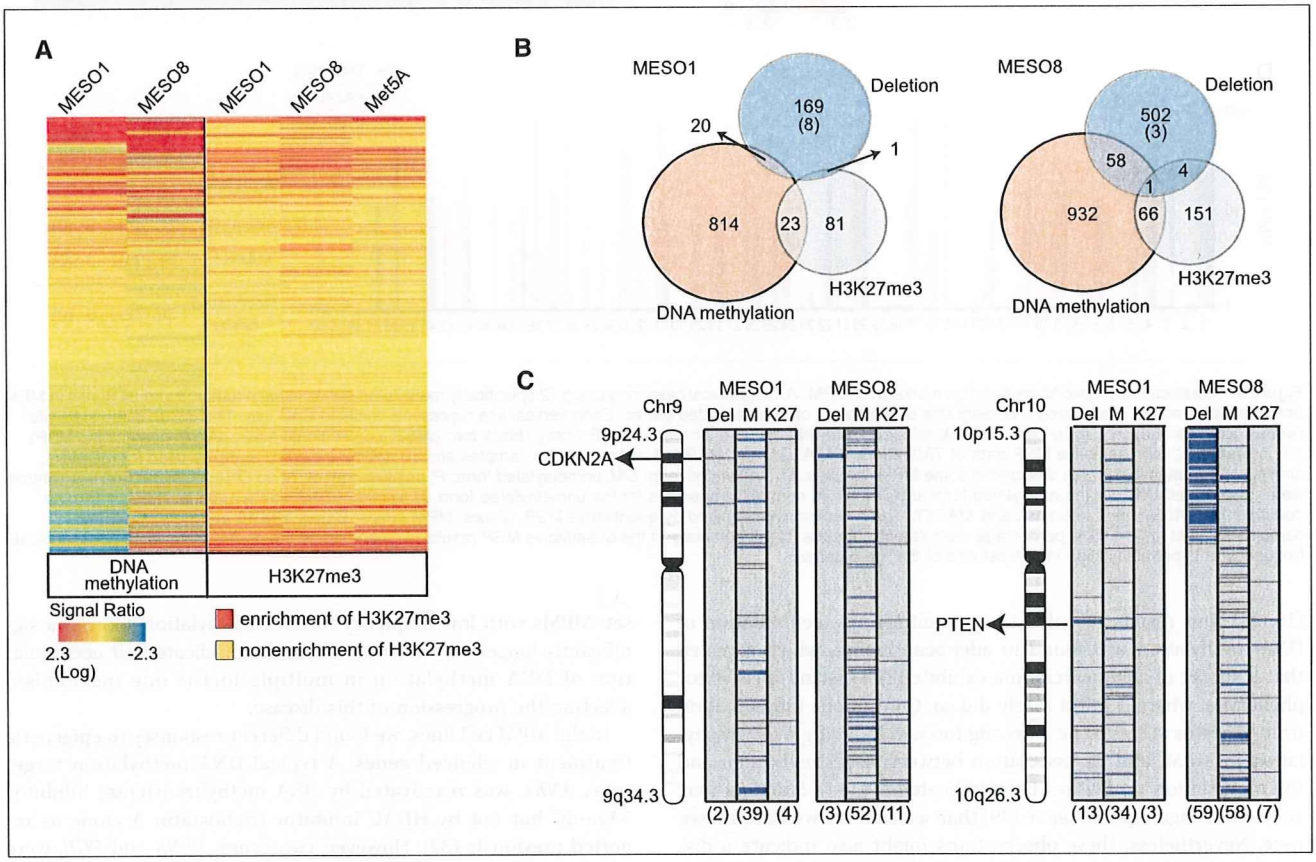

Figure 4. Epigenetic and genetic analysis of MESO1 and MESO8. *A*, unsupervised hierarchical cluster analysis of DNA methylation and H3K27me3 data in two MPM cell lines, MESO1 and MESO8, and a normal mesothelial cell line, MeT-5A, using microarray data of 6,157 genes (*Y axis*). Each cell in the matrix represents the DNA methylation (*red* and *blue*, high and low levels) or H3K27me3 status (*red* and *yellow*, enrichment or nonenrichment of H3K27me3) of each gene in an individual sample. *B*, number of DNA methylation targets, H3K27me3 targets, and deleted genes in MESO1 and MESO8 are shown by Venn diagram. Numbers in parentheses indicate number of homozygously deleted genes. *C*, chromosome view of epigenetic and genetic changes in chromosomes 9 and 10. *Del*, deletion; *M*, DNA methylation; *K27*, H3K27me3. Number of genes involved in each event is shown in parentheses.

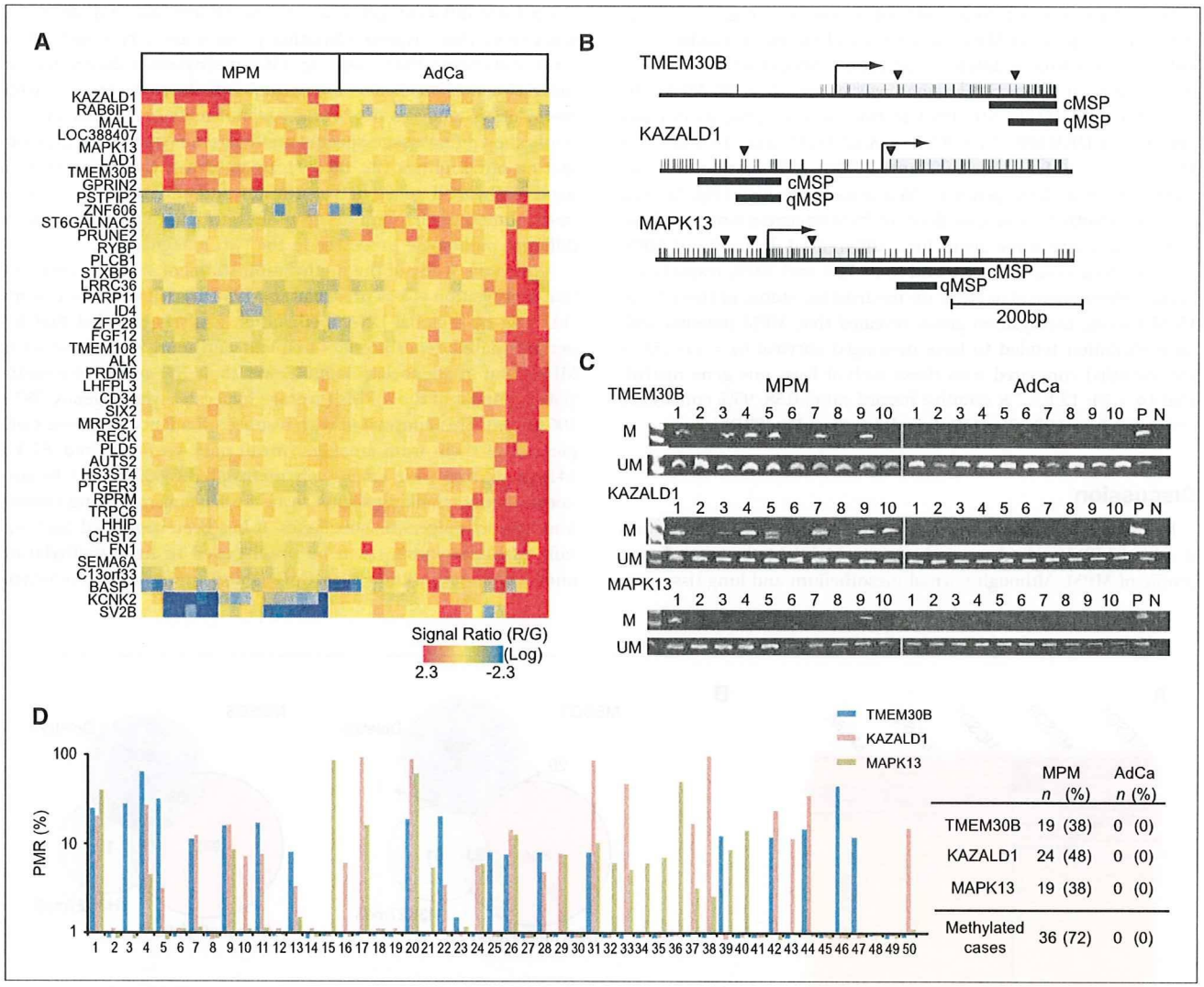

	MPM *n* (%)	AdCa *n* (%)
TMEM30B	19 (38)	0 (0)
KAZALD1	24 (48)	0 (0)
MAPK13	19 (38)	0 (0)
Methylated cases	36 (72)	0 (0)

Figure 5. Identification of specific methylation markers for MPM. *A*, hierarchical clustering using 42 specifically methylated genes in each tumor (8 and 34 genes in MPM and adenocarcinoma, respectively). *B*, diagrams of promoters of three selected genes. Each vertical line represents a single CpG site. The transcription start site (*arrow*), location of exon 1 (*gray box*), *SmaI*/*Xma*I sites (*arrowheads*), and location of MSP assay (*black bar*; *cMSP*, conventional MSP; *qMSP*, quantitative MSP) are indicated. *C*, representative MSP data of *TMEM30B*, *KAZALD1*, and *MAPK13* in the 10 MPM samples and 10 adenocarcinoma samples used for MCAM analysis. DNA methylation was detected in some MPM samples. *M*, methylated form; *UM*, unmethylated form; *P*, positive control; *N*, no DNA template. Positive controls were *Sss*I-treated DNA for the methylated form and DNA from normal lymphocytes for the unmethylated form. *D*, levels of DNA methylation in *TMEM30B* (*blue columns*), *KAZALD1* (*pink columns*), and *MAPK13* (*green columns*) examined by quantitative MSP. *X axis*, MPM cases. Cases 1 to 10 are the same MPM samples as label in *C*. *Y axis*, percentage methylated reference (%). A summary of the quantitative MSP results is given beside the graph. Methylated cases indicate frequency of hypermethylation in at least one of the three genes.

(18, 38). Our results revealed that simultaneous accumulation of DNA methylation was found in adenocarcinoma, which revealed that a subset of adenocarcinoma exhibited CpG island methylator phenotype, whereas MPM rarely did so. Continuous inflammation from asbestos seems to be a driving force in inducing hypermethylation in MPM, and an association between asbestos burden and the methylation profile has been indicated (13, 14). Smoking may act as a stronger epimutagene (39) than asbestos as we have shown here. Nevertheless, these observations might also indicate a distinct mechanism for the acquisition of aberrant DNA methylation during the formation of MPM and adenocarcinoma.

DNA methylation of several genes seems to affect the clinicopathologic phenotype of MPM (40). In this study, we classified MPMs into two groups by methylation profile of a certain gene set; MPMs with low frequency of DNA methylation showed a significantly longer survival rate. These data indicate that accumulation of DNA methylation in multiple loci is one mechanism affecting the progression of this disease.

In the MPM cell lines, we found different responses to epigenetic treatment in silenced genes. A typical DNA methylation target gene, *ANK1*, was reactivated by DNA methyltransferase inhibitor 5Aza-dC but not by HDAC inhibitor trichostatin A alone as reported previously (32). However, two genes, *PENK* and *PGR*, were reactivated by both 5Aza-dC and trichostatin A. Examination of another epigenetic silencing mechanism, H3K27me3, might explain the intricate situation of gene expression in MPMs. When genes are silenced by DNA methylation alone, 5Aza-dC efficiently reactivates the gene; however, trichostatin A is inert in this situation.

When genes are silenced by H3K27me3, both trichostatin A and 5Aza-dC affect gene activity regardless of DNA methylation status. This is consistent with the recent genome-wide analyses of polycomb group–mediated H3K27me3 silencing machinery in prostate cancers showing that a particular set of genes is dominantly silenced by H3K27me3 independent of DNA methylation and can be reactivated by a HDAC inhibitor (21, 41). The reason why silenced *PGR* without DNA methylation was reactivated by 5Aza-dC is not clear (MESO1 in Fig. 3*B*). This might be explained by the several studies suggesting that 5Aza-dC can act independently of its ability to inhibit DNA methylation, inducing the activation of unmethylated genes (42–44).

Integrated analysis of DNA methylation, H3K27me3, and array comparative genomic hybridization data in 5,746 genes in MPM cell lines has revealed that DNA methylation is a major silencing mechanism in CpG promoters and that H3K27me3 regulates a subset of genes, whereas deletions of loci are less frequent. By virtue of this combined analysis, we discovered that, on CpG promoter regions, ~11% of genes were affected by both genetic and epigenetic alterations in MPM, which generally results in their being silenced. These data indicate that multiple epigenetic abnormalities may work in harmony with genetic defects to inactivate a tumor suppressor gene through Knudson's two-hits model, in which a mutation or heterozygous deletion combines with DNA methylation and/or H3K27me3 to inactivate two alleles. Clinical trials using a different HDAC inhibitor, suberoylanilide hydroxamic acid, have been conducted in recurrent MPMs, but that drug is ineffective for the treatment of this disease (45). This might be partially explained by evidence showing that the HDAC inhibitor could not reactivate the genes silenced by DNA methylation. Taken together, our data suggest that the targeting DNA methylation in addition to H3K27me3 might be of great benefit and could improve the treatment of MPM.

DNA methylation has been proposed as a powerful marker for MPM diagnosis (11, 12). However, a previous examination of the methylation status of both MPM and adenocarcinoma showed that hypermethylation of the candidate markers was detected in both MPMs and adenocarcinomas to some extent, although at different frequencies. In addition, methylation markers specific for MPM have not been reported previously. Our analysis showed that hypermethylation of certain loci was frequently detected in MPM and that three genes in particular, *TMEM30B* (46), *KAZALD1* (47), and *MAPK13* (48), were specifically methylated in MPM. Their aberrant methylation could serve as informative markers to distinguish MPMs from adenocarcinomas and could be applicable for the samples obtained from less invasive procedures, such as serum and pleural effusion. A larger study is needed to validate these three genes as useful diagnostic markers for MPM.

In summary, a global methylation analysis comparing MPM and adenocarcinoma can decipher characteristic DNA methylation patterns in MPM. Because multiple epigenetic abnormalities might contribute to tumorigenesis through the silencing of particular cancer-related genes, targeting these epigenetic mechanisms could potentially be effective treatments for clinical use in MPM. Finally, here we propose potential markers that could be of diagnostic value for use in MPMs.

Disclosure of Potential Conflicts of Interest

No potential conflicts of interest were disclosed.

Acknowledgments

Received 4/30/09; revised 8/27/09; accepted 9/15/09; published OnlineFirst 11/3/09.

Grant support: Special Coordination Fund for Promoting Science and Technology from the Ministry of Education, Culture, Sports, Science and Technology of Japan (H18-1-3-3-1; Y. Sekido); Grant-in-Aid for Scientific Research from the Japan Society for the Promotion of Science (Y. Sekido, Y. Kondo); Third-Term Comprehensive Control Research for Cancer and Grant-in-Aid for Cancer Research from the Ministry of Health, Labor, and Welfare (Y. Sekido, Y. Kondo); and 24th General Assembly of the Japanese Association of Medical Sciences (Y. Kondo).

The costs of publication of this article were defrayed in part by the payment of page charges. This article must therefore be hereby marked *advertisement* in accordance with 18 U.S.C. Section 1734 solely to indicate this fact.

We thank Ikuko Tomimatsu and Shoko Mitsumatsu for technical assistance and Shana Straub for critical reading of the article.

MIAME accession numbers: Array Express: E-TABM-813 (MCAM data of 20 MPMs and 20 adenocarcinomas), E-TABM-781 (chromatin immunoprecipitation-microarray in MPM cells), and E-TABM-808 (MCAM data in MPM cells).

References

1. Robinson BW, Lake RA. Advances in malignant mesothelioma. N Engl J Med 2005;353:1591–603.
2. Tsiouris A, Walesby RK. Malignant pleural mesothelioma: current concepts in treatment. Nat Clin Pract Oncol 2007;4:344–52.
3. van Meerbeeck JP, Gaafar R, Manegold C, et al. Randomized phase III study of cisplatin with or without raltitrexed in patients with malignant pleural mesothelioma: an intergroup study of the European Organisation for Research and Treatment of Cancer Lung Cancer Group and the National Cancer Institute of Canada. J Clin Oncol 2005;23:6881–9.
4. Cheng JQ, Jhanwar SC, Klein WM, et al. p16 alterations and deletion mapping of 9p21-22 in malignant mesothelioma. Cancer Res 1994;54:5547–51.
5. Sekido Y, Pass HI, Bader S, et al. Neurofibromatosis type 2 (NF2) gene is somatically mutated in mesothelioma but not in lung cancer. Cancer Res 1995;55:1227–31.
6. Bianchi AB, Mitsunaga SI, Cheng JQ, et al. High frequency of inactivating mutations in the neurofibromatosis type 2 gene (NF2) in primary malignant mesotheliomas. Proc Natl Acad Sci U S A 1995;92:10854–8.
7. Sugarbaker DJ, Richards WG, Gordon GJ, et al. Transcriptome sequencing of malignant pleural mesothelioma tumors. Proc Natl Acad Sci U S A 2008;105:3521–6.
8. Krismann M, Muller KM, Jaworska M, Johnen G. Molecular cytogenetic differences between histological subtypes of malignant mesotheliomas: DNA cytometry and comparative genomic hybridization of 90 cases. J Pathol 2002;197:363–71.
9. Jones PA, Baylin SB. The fundamental role of epigenetic events in cancer. Nat Rev Genet 2002;3:415–28.
10. Perwez Hussain S, Harris CC. Inflammation and cancer: an ancient link with novel potentials. Int J Cancer 2007;121:2373–80.
11. Toyooka S, Pass HI, Shivapurkar N, et al. Aberrant methylation and simian virus 40 tag sequences in malignant mesothelioma. Cancer Res 2001;61:5727–30.
12. Tsou JA, Shen LY, Siegmund KD, et al. Distinct DNA methylation profiles in malignant mesothelioma, lung adenocarcinoma, and non-tumor lung. Lung Cancer 2005;47:193–204.
13. Tsou JA, Galler JS, Wali A, et al. DNA methylation profile of 28 potential marker loci in malignant mesothelioma. Lung Cancer 2007;58:220–30.
14. Christensen BC, Houseman EA, Godleski JJ, et al. Epigenetic profiles distinguish pleural mesothelioma from normal pleura and predict lung asbestos burden and clinical outcome. Cancer Res 2009;69:227–34.
15. Xu L, Flynn BJ, Ungar S, et al. Asbestos induction of extended lifespan in normal human mesothelial cells: interindividual susceptibility and SV40 T antigen. Carcinogenesis 1999;20:773–83.
16. Bocchetta M, Di Resta I, Powers A, et al. Human mesothelial cells are unusually susceptible to simian virus 40-mediated transformation and asbestos cocarcinogenicity. Proc Natl Acad Sci U S A 2000;97:10214–9.
17. Yang H, Bocchetta M, Kroczynska B, et al. TNF-α inhibits asbestos-induced cytotoxicity via a NF-κB-dependent pathway, a possible mechanism for asbestos-induced oncogenesis. Proc Natl Acad Sci U S A 2006;103:10397–402.
18. Toyota M, Ahuja N, Ohe-Toyota M, Herman JG, Baylin SB, Issa JP. CpG island methylator phenotype in colorectal cancer. Proc Natl Acad Sci U S A 1999;96:8681–6.
19. Kirmizis A, Bartley SM, Kuzmichev A, et al. Silencing of human polycomb target genes is associated with methylation of histone H3 Lys 27. Genes Dev 2004;18:1592–605.
20. van der Vlag J, Otte AP. Transcriptional repression mediated by the human polycomb-group protein EED involves histone deacetylation. Nat Genet 1999;23:474–8.
21. Kondo Y, Shen L, Cheng AS, et al. Gene silencing in cancer by histone H3 lysine 27 trimethylation independent of promoter DNA methylation. Nat Genet 2008;40:741–50.

22. Shen L, Kondo Y, Guo Y, et al. Genome-wide profiling of DNA methylation reveals a class of normally methylated CpG island promoters. PLoS Genet 2007;3:2023–36.
23. Gao W, Kondo Y, Shen L, et al. Variable DNA methylation patterns associated with progression of disease in hepatocellular carcinomas. Carcinogenesis 2008;29: 1901–10.
24. Usami N, Fukui T, Kondo M, et al. Establishment and characterization of four malignant pleural mesothelioma cell lines from Japanese patients. Cancer Sci 2006; 97:387–94.
25. Eisen MB, Spellman PT, Brown PO, Botstein D. Cluster analysis and display of genome-wide expression patterns. Proc Natl Acad Sci U S A 1998;95:14863–8.
26. Yang AS, Estecio MR, Doshi K, Kondo Y, Tajara EH, Issa JP. A simple method for estimating global DNA methylation using bisulfite PCR of repetitive DNA elements. Nucleic Acids Res 2004;32:e38.
27. Kondo Y, Shen L, Suzuki S, et al. Alterations of DNA methylation and histone modifications contribute to gene silencing in hepatocellular carcinomas. Hepatol Res 2007;37:974–83.
28. Shen L, Guo Y, Chen X, Ahmed S, Issa JP. Optimizing annealing temperature overcomes bias in bisulfite PCR methylation analysis. Biotechniques 2007;42:48, 50, 2 passim.
29. Eads CA, Lord RV, Wickramasinghe K, et al. Epigenetic patterns in the progression of esophageal adenocarcinoma. Cancer Res 2001;61:3410–8.
30. Kondo Y, Shen L, Issa JP. Critical role of histone methylation in tumor suppressor gene silencing in colorectal cancer. Mol Cell Biol 2003;23:206–15.
31. Ogino S, Cantor M, Kawasaki T, et al. CpG island methylator phenotype (CIMP) of colorectal cancer is best characterised by quantitative DNA methylation analysis and prospective cohort studies. Gut 2006;55: 1000–6.
32. Cameron EE, Bachman KE, Myohanen S, Herman JG, Baylin SB. Synergy of demethylation and histone deacetylase inhibition in the re-expression of genes silenced in cancer. Nat Genet 1999;21:103–7.
33. Taniguchi T, Karnan S, Fukui T, et al. Genomic profiling of malignant pleural mesothelioma with array-based comparative genomic hybridization shows frequent non-random chromosomal alteration regions including JUN amplification on 1p32. Cancer Sci 2007; 98:438–46.
34. Flotho C, Paulun A, Batz C, Niemeyer CM. AKAP12, a gene with tumour suppressor properties, is a target of promoter DNA methylation in childhood myeloid malignancies. Br J Haematol 2007;138:644–50.
35. Belinsky SA. Gene-promoter hypermethylation as a biomarker in lung cancer. Nat Rev Cancer 2004;4:707–17.
36. Estecio MR, Yan PS, Ibrahim AE, et al. High-throughput methylation profiling by MCA coupled to CpG island microarray. Genome Res 2007;17:1529–36.
37. Weber M, Hellmann I, Stadler MB, et al. Distribution, silencing potential and evolutionary impact of promoter DNA methylation in the human genome. Nat Genet 2007;39:457–66.
38. Suzuki M, Shigematsu H, Iizasa T, et al. Exclusive mutation in epidermal growth factor receptor gene, HER-2, and KRAS, synchronous methylation of non-small cell lung cancer. Cancer 2006;106:2200–7.
39. Grady WM. CIMP and colon cancer gets more complicated. Gut 2007;56:1498–500.
40. Fischer JR, Ohnmacht U, Rieger N, et al. Promoter methylation of RASSF1A, RARβ and DAPK predict poor prognosis of patients with malignant mesothelioma. Lung Cancer 2006;54:109–16.
41. Gal-Yam EN, Egger G, Iniguez L, et al. Frequent switching of Polycomb repressive marks and DNA hypermethylation in the PC3 prostate cancer cell line. Proc Natl Acad Sci U S A 2008;105:12979–84.
42. Milutinovic S, Knox JD, Szyf M. DNA methyltransferase inhibition induces the transcription of the tumor suppressor p21(WAF1/CIP1/sdi1). J Biol Chem 2000; 275:6353–9.
43. Soengas MS, Capodieci P, Polsky D, et al. Inactivation of the apoptosis effector Apaf-1 in malignant melanoma. Nature 2001;409:207–11.
44. Wozniak RJ, Klimecki WT, Lau SS, Feinstein Y, Futscher BW. 5-Aza-2′-deoxycytidine-mediated reductions in G9A histone methyltransferase and histone H3 K9 di-methylation levels are linked to tumor suppressor gene reactivation. Oncogene 2007;26:77–90.
45. Ramalingam SS, Belani CP, Ruel C, et al. Phase II study of belinostat (PXD101), a histone deacetylase inhibitor, for second line therapy of advanced malignant pleural mesothelioma. J Thorac Oncol 2009;4: 97–101.
46. Furuta J, Nobeyama Y, Umebayashi Y, Otsuka F, Kikuchi K, Ushijima T. Silencing of peroxiredoxin 2 and aberrant methylation of 33 CpG islands in putative promoter regions in human malignant melanomas. Cancer Res 2006;66:6080–6.
47. Shibata Y, Tsukazaki T, Hirata K, Xin C, Yamaguchi A. Role of a new member of IGFBP superfamily, IGFBP-rP10, in proliferation and differentiation of osteoblastic cells. Biochem Biophys Res Commun 2004;325: 1194–200.
48. Ehrlich M, Sanchez C, Shao C, et al. ICF, an immunodeficiency syndrome: DNA methyltransferase 3B involvement, chromosome anomalies, and gene dysregulation. Autoimmunity 2008;41:253–71.